

## High-intensity Focused Ultrasound: preliminary experiences

Martínez V. Raquel, Vera H. Arturo, Leija S. Lorenzo

Department of Electrical Engineering, Bioelectronics Section,  
CINVESTAV-IPN, Av. Instituto Politécnico Nacional No. 2508,  
México D. F. 07360  
laremus@cinvestav.mx

### Abstract

Ultrasonic thermal ablation is being used nowadays for causing coagulative necrosis within the body by increasing tissue temperature over  $56^{\circ}\text{C}$  denoting high-intensity focused ultrasound (HIFU) as a technology for selective tissue ablation. HIFU effects can be observed in a tissue-mimicking material (phantom). An electrical system for exciting HIFU transducer mainly consists of: sinusoidal wave generator, radiofrequency amplifier, power meter and HIFU transducer. An oscillator based on direct digital synthesis was designed. Its principal specifications include frequency and amplitude stability, low harmonic distortion and frequency adjustment with 1 kHz resolution. In this work, it is presented the electrical system performance, temperature measurements made in phantom and a thermo-acoustic finite element model of a HIFU transducer. Acoustic field and temperature numerical simulation were validated with measurements.

**Keywords:** finite element modeling, HIFU, focused ultrasound, oncology, thermal ablation

**PACS no.** 43.58.Wc, 43.80.Vj, 43.10.Ce

## 1 Introduction

High intensity focused ultrasound (HIFU) is a non invasive technique used for provoking thermal ablation within a target, *i.e.* oncological tumors. Ultrasonic beam can be focused by using spherical and rectangular concave transducers or element arrays. This focalization results in an energy concentration in a millimetric cigar shape focus. Acoustic intensity increases at the focus generating a temperature raise over  $56^{\circ}\text{C}$  that causes irreversible cell damage in a few seconds. The absorption of ultrasonic energy causes rapid temperature increase over  $50^{\circ}\text{C}$  and focalization minimizes surrounding tissue damage [1]. Tissue thermal coagulation is immediate and relatively independent of non-homogeneous media and tissue thermal parameters such as blood perfusion [2, 3]. For treatment of large volumes, interval in the order of 30 s to 60 s between each exposure may be required to avoid temperature buildup or accumulation of thermal dose in non intended regions [3]. Different configurations and devices (such as extracorporeal, interstitial and transrectal devices) are being used to treat breast cancer, uterine fibroids, liver cancer, pancreatic cancer, kidney cancer, benign prostatic hyperplasia (BPH) and prostatic cancer [3-8].

In order to deliver HIFU energy, a transducer has to be excited. Depending on the device design, electrical power and signal amplification are required. HIFU transducers are usually excited with sinusoidal continuous or pulsed waveforms. Signal generators usually present a low power output;

nevertheless, radiofrequency (RF) amplifiers can be used to amplify the signal to drive the HIFU transducer. A power meter is necessary to verify system coupling by measuring the standing wave ratio (SWR) between the RF amplifier and the HIFU transducer.

Overall electrical system characterization and HIFU transducer response is required before making any experimental trial. In this paper we report part of our first experiences by using high intensity focused ultrasound such as excitation system design, transducer acoustic characterization, focal temperature measurement and thermo-acoustic finite element modeling of a concave spherical transducer with 1.965 MHz operating frequency.

## 2 Methodology

### 2.1 Electrical system

In order to excite the HIFU transducer, a sinusoidal wave generator based on direct digital synthesizer (DDS) was designed with a programmable bandwidth from 1 MHz to 10 MHz. Low harmonic distortions, impedance matching, and frequency and amplitude stability were the most important required characteristics [10, 11]. Previous work developed at our laboratory showed that these requirements should be satisfied [9, 10, 11].

Figure 1 shows the HIFU system diagram connection. A virtual interface was designed to set up the oscillation frequency and control the DDS generator output amplitude [11]. Then, sinusoidal signal is amplified 50 dB by the RF amplifier KMA1040® which presents plane amplification in the band pass. A power meter measured the electrical incident and reflected wave between the RF amplifier and the HIFU transducer's impedance matching network (IMN). Finally, degassed water is used as coupling medium between the concave transducer and the target.

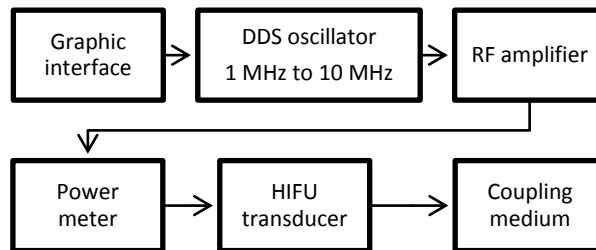


Figure 1. Block diagram for electrical system setup.

### 2.2 Field characterization

Acoustic distribution was performed by fixing the transducer inside a degassed water tank. A calibrated hydrophone acquired the electrical response corresponding to the acoustic pressure at each point by using a high resolution 3D positioning system. A Tektronix AFG3021B function generator excited the HIFU transducer with a 1.965 MHz/ 10 Vpp burst with a repetition frequency of 10 Hz. Hydrophone PVPF-Z44-0440 swept X and Y axis with a resolution of 0.1016 mm, while Z axis was swept with a resolution of 1 mm with Scan 3.40 3D positioning system. Data was stored by the Waveform® software. The disadvantage of this technique is that it is performed at low acoustic power levels compared to those used in oncological applications to avoid damaging the hydrophone [10].

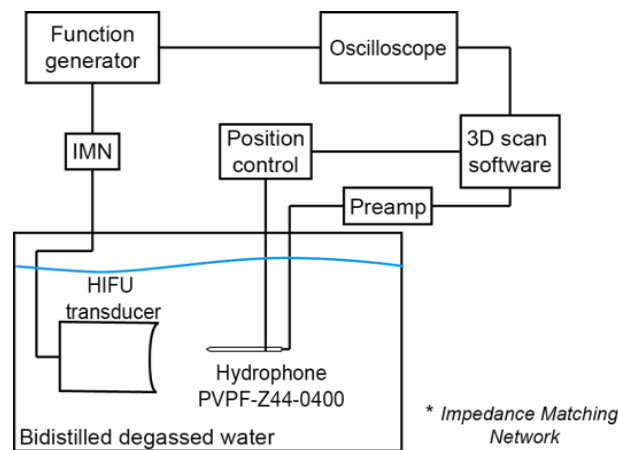


Figure 2. HIFU transducer acoustic characterization

### 2.3 Focal temperature measurements in phantom

The experiment consisted on exciting the HIFU transducer at a continuous sine wave of 1.965 MHz with an electrical power of 50 W for 3 min. A graphical interface was used to set the transducer operating frequency, and an attenuator was used as protection for the commercial amplifier which maximum input power is 1 Mw. A continuous sinusoidal wave was amplified 50 dB by the radiofrequency amplifier. A power meter measured constantly the incident and reflected power in the connection between the RF amplifier and the HIFU transducer during the whole experiment, resulting in a SWR of 1.08. Exciting electrical power was initially set at 2 W for 10 s, and then it was incremented linearly from 2 W to 50 W during the next 30 s; finally, it stayed constant at 50 W the rest of the time to complete 200 s. Temperature increments were measured with a thermocouple placed at the focus ( $z=17\text{mm}$ ) within a tissue-mimicking material [10] which acted as an absorber of ultrasonic energy (see Figure 3). Distilled-degassed water was used as ultrasonic coupling media; which was temperature regulated at  $37^\circ\text{C}$ . Temperature data during HIFU exposure were stored each second in a digital multimeter for post-processing use.

### 2.4 Thermo-acoustic field modeling

#### 2.4.1 Acoustic model

The finite element (FE) model was developed based on the cylindrical coordinate system  $(r, z)$  where the transducer was located at  $z=0$  and the radiation propagated in the  $z$ -direction. The boundaries were defined in accordance with the experimental setup. The acoustic transducer was simulated as a membrane which acted as an acoustic radiator. In figure 4, boundary 5 was configured as to represent the concave transducer. Boundary 10 was simulated as an acoustically rigid wall by setting the normal velocity at zero. Boundary 1, 2, 3, and 4 were the propagation axis of the problem. Boundaries 9 and 12 had the same acoustic impedance as the media ( $Z = \rho c$ ) to avoid wave reflections. Boundaries 6, 7, 8, and 11 were configured with the acoustic continuity condition to permit free-wave propagation [12]. The FE mesh for acoustic model consisted of 27 403 squared and triangular elements, three per wavelength. The finite element model is made on a 2D axisymmetric geometry using the physical characteristics of the transducer, such as radius of the circular boundary  $a = 10\text{ mm}$  and the depth of the concave surface  $h = 3\text{ mm}$ , radiating on a lossless media (water).

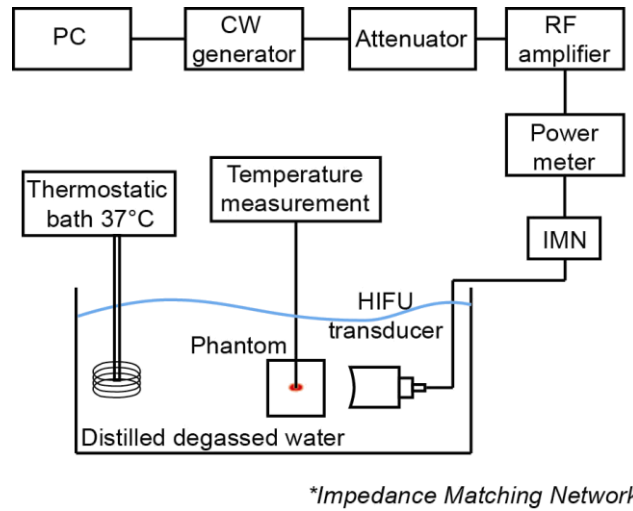


Figure 3. Focal temperature measurement in phantom

The dimensions of the geometry, subdomain or medium 20 cm x 40 cm, were set in order to compare the results obtained with the data acquired from pressure measurements. The frequency was set at 1.965 MHz and the ultrasound velocity in the medium was defined as 1500 m/s<sup>2</sup> which is nearly the speed of ultrasound in water at 25°C. The density of water was established at 1000 kg/m<sup>3</sup>.

The spatial-peak temporal-average acoustic intensity ( $I_{SPTA}$ ) at the transducer radiating surface was determined from the measurements with the equation [13]:

$$I_{SPTA} = \frac{1}{\rho c} \left( \frac{V_{rms}}{S_{hydrophone}} \right)^2, \quad (1)$$

where  $\rho$  is the medium density,  $c$  is the acoustic wave velocity in the medium,  $V_{rms}$  is the measurement given by the hydrophone in volts rms and  $S_{hydrophone}$  is the hydrophone sensitivity. This intensity measured very close to the transducer radiating surface represents the emitted acoustic intensity  $I_0$  at a specific power. The pressure at the radiator surface was determined by [14]

$$|\rho_0| = \sqrt{\frac{2\rho c I_0}{M}}, \quad (2)$$

where  $|\rho_0|$  is the pressure amplitude at the transducer surface,  $I_0$  is the measured acoustic intensity very close to the transducer surface, and  $M$  is a parameter related to the transducer geometry given by [14]

$$M = \frac{1}{2} \left( \sqrt{(z-h)^2 + a^2} + z \right), \quad (3)$$

with reference to the parameters of figure 4, in which  $Z$  is any point on the propagation axis.

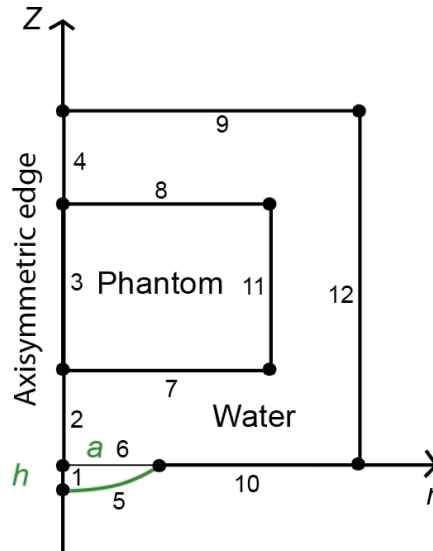


Figure 4. Finite element geometry

### 2.4.2 Heating model

The coordinate system was the same as that of the FE model for the acoustic field. The boundary conditions were chosen in accordance with the experimental setup (see Figure 4). Boundaries 1, 2, 3 and 4 were the symmetry axis, similar to the acoustic field model. Boundary 5 was thermally insulated and it does not permit the heat flow to avoid modification of the thermal distribution due to heat interchange. Boundaries 9, 10, and 12 were configured to have 37 °C, which is the temperature of the water in the experiments (controlled by the thermostatic bath). Boundaries 6, 7, 8, and 11 were configured to have a continuity condition among the adjacent subdomains to permit a complete thermal interchange.

Concerning the relation of ultrasound and temperature, the time average heat  $Q$  produced in media depends on both the intensity  $I$  and the pressure amplitude absorption coefficient  $\alpha$ , as  $Q = 2\alpha I$  [15]; here, the nonlinear absorption was not accounted. Also, it was considered that all the attenuation was due to absorption and that the scattering effect was negligible. Subsequently, the temperature distribution  $T$  in the medium was obtained by the Pennes bioheat equation, with no contribution of metabolism and blood flow:

$$\rho C \frac{\partial T}{\partial t} - \bar{k} \nabla^2 T = Q_{ext}, \quad (4)$$

where  $\rho$  is the medium density,  $C$  is the medium heat capacity,  $\bar{k}$  is the phantom thermal conductivity, and  $Q_{ext}$  is the heat produced by an external source which is related to the acoustic intensity as explained above. Metabolism and blood flow were omitted from Pennes bioheat equation because the HIFU energy was applied to a phantom.

The stable-state solution for pressure in attenuation-free media was used as the input of the heating problem employing  $Q_{ext}$ .

### 3 Results

#### 3.1 Electrical system performance

Electrical system characterization consisted of measuring the frequency and amplitude in a certain period of time every second for 30 min and 60 min, respectively. DDS-oscillator was programmed to generate a 1.965 MHz sinusoidal frequency. Figure 5 shows the corresponding parameter measurement. The standard deviations were calculated, obtaining a deviation of 0.0 Hz for the frequency measurement and 12.40 mVpp amplitude deviation [11].

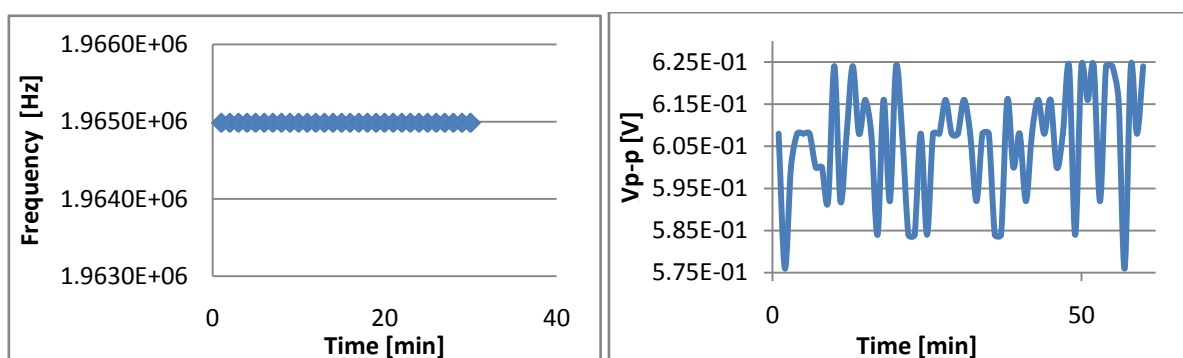


Figure 5. DDS-oscillator frequency (left) and amplitude (right) stability at 1.965 MHz. Frequency standard deviation was found to be 0.0 Hz. Amplitude standard deviation was found to be 12.40 mVpp

Sinusoidal generated signal frequency contain was observed by using a spectrum analyzer. In figure 6, it can be seen that the higher peak is placed at 1.965 MHz and had amplitude of -5 dBm, approximately. The second peak is placed at 4 MHz approximately and presented amplitude of -42 dBm. Signal generation comes along with alias generation at  $n = 1, 2, 3 \dots$ , of the fundamental frequency. In high power excitation systems, the presence of harmonics may influence the power reflected during excitation in the same way that an impedance mismatch varies the power transference in a transmission line. Total harmonic distortion (*THD*) is a parameter to evaluate the presence of fundamental frequency alias by the following equation:

$$THD[dB] = 20 \log_{10} \left( \sqrt{\frac{V_2^2 + V_3^2 + V_4^2 + V_5^2 + V_6^2}{V_1^2}} \right), \quad (5)$$

where  $V_2, V_3, V_4, V_5$  y  $V_6$  are the rms (root mean square) voltages amplitudes from the second to sixth harmonic and  $V_1$  is the rms voltage of the fundamental frequency.

Total harmonic distortion obtained at 1.965 MHz was -45.72 dB.

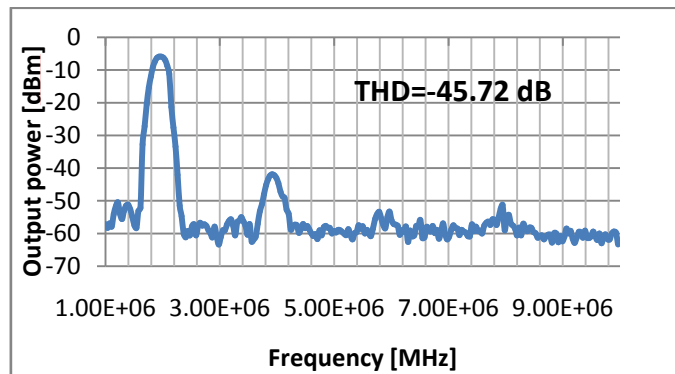


Figure 6. DDS-oscillator harmonic distortion at 1.965 MHz.

Radiofrequency amplifier response at the band pass from 1 MHz to 10 MHz is shown in figure 7. Output power variation observed was of 5 W from the extremes of the frequency range.

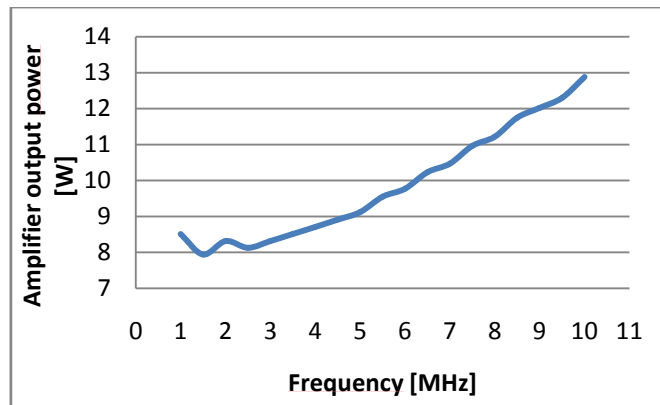


Figure 7. Radiofrequency amplifier output power vs frequency

### 3.2 Acoustic field characterization vs model comparison

Figure 8 shows both the acoustic field measurement made by using a hydrophone and the acoustic field modeled by finite element method. Normalized acoustic distribution is shown in order to compare the HIFU acoustic pattern. HIFU field measurement was done with a resolution of 0.1016 mm in both X and Y axis and a resolution of 1 mm in the propagation axis Z. Nevertheless both measured and simulated acoustic fields show a good concordance in the acoustic distribution. For both graphics, it can be seen that the point with mayor intensity concentration is at 17 mm.

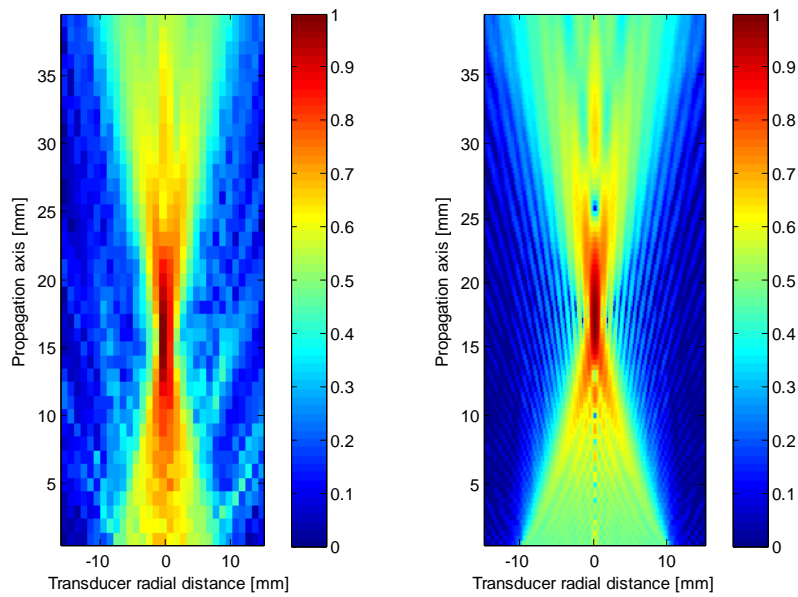


Figure 8. Normalized acoustic distribution: measured (left) and modeled (right)

### 3.3 Temperature increase curve comparison

The modeled temperature increments at the focus are compared with the measured ones (see figure 9, left graphic). This graph indicates great concordance for this application between modeled and measured temperature increments. The measured data were affected by thermocouple movements due to vibration provoked by the high intensity acoustic pressure.

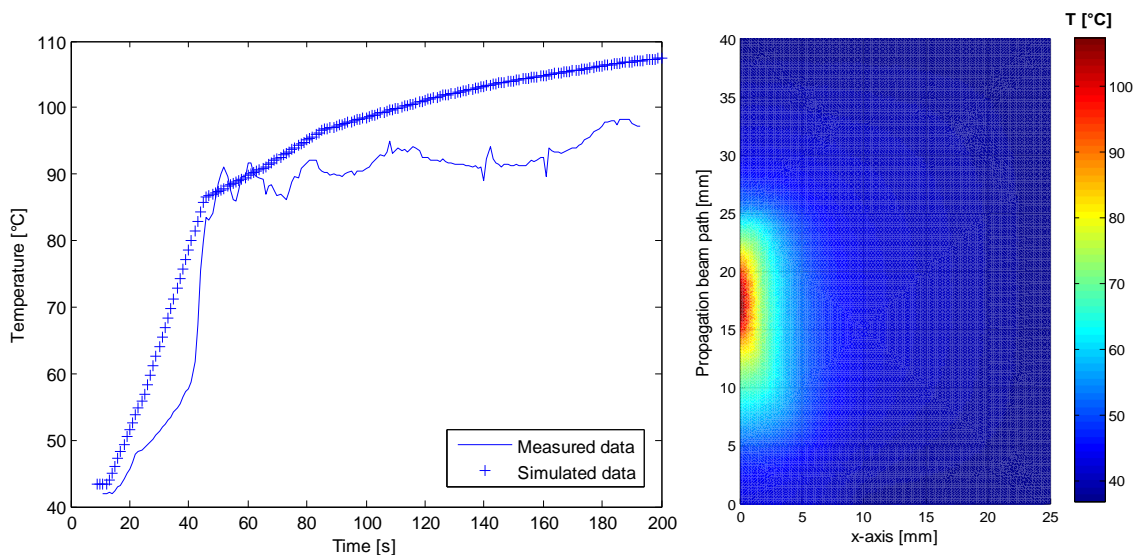


Figure 9. Modeled and measured temperature at the focus (left). Temperature distribution modeled after 200 s (right).

The modeled temperature distribution inside the tissue-mimicking material is shown in right hand side of figure 9 and it shows that the hottest point is located at 17 mm which is the HIFU transducer focal depth.

## 4 Discussion and Conclusion

A DDS-oscillator was designed to accomplish with high frequency and amplitude stability, low harmonic distortion which serves to reduce the reflected power that can damage both the HIFU transducer and the RF amplifier. All these requirements have been studied for our workgroup earlier [10, 11]

Acoustic field and temperature increase due to the phantom ultrasound absorption has been simulated in an axisymmetric model. HIFU transducer parameters such as radius and curvature have been included in the numerical simulation. Phantom acoustic characteristic and temperature measurement conditions were taken into account. Although figures 8 and 9 show great result congruency it has to be denoted that non-linear effects were taken into account during acoustic field and temperature simulations. Transducer acoustic field characterization is made at low power and then data are extrapolated to higher acoustic power [16]. Heating differences at the focal region may also be caused by neglecting the non-linear effects of high power acoustics. Temperature measured data presented variations that could be the influence of cavitation and viscous heating artifact [17]. Phantom exposure time to HIFU energy could be shortening in order to avoid phantom heating by thermal conduction and interfere with real temperature measurement in that specific point. It also should be manufactured in order to improve its thermal properties [17], because for these experiments it was also taken into account the ultrasonic propagation speed.

### Acknowledgment

Authors thank the financial support of the CINVESTAV-IPN, CONACYT project number 68799, the project of the program ECOS-ANUIES-CONACYT M10-S02, the ICyTDF project PICCO10-78.

### References

- [1] Dubinsky, T.J.; Cuevas, C.; Dighe, M. K.; Kolokythas, O.; Hwang, J. H. High-intensity focused ultrasound: Current potential and oncologic applications. *American Journal of Roentgenology*, 190(1), 2008, 191-199.
- [2] ter Haar, G.; Coussios, C. High intensity focused ultrasound: past, present and future. *International Journal of Hyperthermia*, 23(2),2007,85-7.
- [3] Diederich, C. J.; Hynynen, K. Ultrasound technology for hyperthermia. *Ultrasound in Medicine and Biology*, 25(6), 1999, 871-887.
- [4] ter Haar, G.; Coussios, C. High intensity focused ultrasound: physical principles and devices. *International Journal of Hyperthermia*, 23(2), 2007, 89-104.
- [5] Kennedy, J. E.; ter Haar, G. R.; Cranston, D. High intensity focused ultrasound: surgery or the future? *The British Journal of Radiology*, 76(909), 2003, 590-9.
- [6] Hwang, J. H.; Crum, L. A. Current status of clinical high-intensity focused ultrasound. *Conf Proc IEEE Eng Med Biol Soc*,1, 2009, 130-3.
- [7] Illing, R.; Champan, A. The clinical applications of high intensity focused ultrasound in the prostate. *International Journal of Hyperthermia* 23(2), 2007, 183-191.
- [8] ter Haar, G. Therapeutic ultrasound. *European Journal of Ultrasound*, 9(1), 1999, 3-9.

- [9] Vera, A.; Leija, L.; Muñoz, R.; Vives A. A. *Ultrasonic hyperthermia*. Springer-Verlag Berlin Heidelberg, Berlin, 2008.
- [10] Martínez, R.; Vera, A.; Leija, L. Portable and tunable continuous wave driver from 1 MHz to 10 MHz for HIFU transducers. *Health Care Exchanges (PAHCE), 2011 Pan American*, Rio de Janeiro, Brasil, march 28- april 1 2011, 122-126.
- [11] Alí, J. M.; Teja, J. L.; García, F. M.; Vera, A.; Leija, L. Dispositivo de baja distorsión armónica y alta estabilidad en frecuencia y amplitud para la excitación de transductores HIFU: validación del dispositivo y pruebas en phantom. *XXXV Congreso Nacional de Ingeniería Biomédica (CNIB2012)*, San Luis Potosí, México, 2012, *accepted*.
- [12] Gutiérrez, M. I.; Vera, A.; Leija, L. Finite element modeling of acoustic field of physiotherapy ultrasonic transducer and the comparison with measurements. *Health Care Exchanges (PAHCE), 2010 Pan American*, Lima, Perú, march 15-19, 2010, 76-80.
- [13] Chen, D.; Fan, T.; Zhang, D.; Wu, J. A feasibility study of temperature rise measurement in a tissue phantom as an alternative way for characterization of the therapeutic high intensity focused ultrasonic field. *Ultrasonics*, 49(8), 2009, 733-42.
- [14] O'Neil, H. T. Theory of focusing radiators. *Journal of the Acoustical society of America*. 21(5), 1949, 516-526.
- [15] Moros, E. G.; Dutton, A. W.; Roedmer, R. B.; Burton, M.; Hynynen, K. Experimental evaluation of two simple thermal models using hyperthermia in muscle in vivo. *International Journal of Hyperthermia*, 9(4), 1993, 581-98.
- [16] Shaw, A.; ter Haar, G. R. *Requirements for measurements standards in High Intensity Focused Ultrasound (HIFU) fields*. National Physical Laboratory (NPL), 2006.
- [17] Maruvada, S.; Liu, Y.; Pritchard, W. F.; Herman, B. A.; Harris, G. R. Comparative study of temperature measurements in ex vivo swine muscle and a tissue-mimicking material during high intensity focused ultrasound exposures. *Phys Med Biol*, 57(1), 1-19.